Article

Enhanced photoelectrochemical method for sensitive detection of protein kinase A activity using TiO/g-CN, PAMAM dendrimer and alkaline phosphatase

Xue Li, Lusheng Zhu, Yunlei Zhou, Huanshun Yin, and Shiyun Ai

Anal. Chem., **Just Accepted Manuscript** • DOI: 10.1021/acs.analchem.6b04184 • Publication Date (Web): 23 Jan 2017

Enhanced photoelectrochemical method for sensitive detection of protein kinase A activity using TiO_2/g-C_3N_4, PAMAM dendrimer and alkaline phosphatase

Xue Li [a], Lusheng Zhu [b], Yunlei Zhou [a], Huanshun Yin [a,*], Shiyun Ai [a,*]

a College of Chemistry and Material Science, Shandong Agricultural University, Taian, 271018, P. R. China.

b College of Resources and Environment, Shandong Agricultural University, Taian, 271018, P. R. China.

* Corresponding authors:

E-mail address: yinhs@sdau.edu.cn (Huanshun Yin); ashy@sdau.edu.cn (Shiyun Ai).

Abstract: A novel photoelectrochemical (PEC) assay is developed for sensitive detection of protein kinase A (PKA) activity based on PKA-catalyzed phosphorylation reaction in solution and signal amplification strategy triggered by PAMAM dendrimer and alkaline phosphatase (ALP). In this strategy, it is noteworthy at this point that PKA phosphorylation was achieved in solution instead of on the surface of the electrode, which has advantages of the good contact in reactants and simple experimental procedure. For immobilizing the phosphorylated peptide (P-peptide) on electrode surface, graphite-like carbon nitride (g-C_3N_4) and titanium dioxide (TiO_2) complex is synthesized and characterized, which plays a significant role for TiO_2 conjugating phosphate groups and g-C_3N_4 providing PEC signal. Subsequently, PAMAM dendrimer and ALP can be captured on P-peptide and TiO_2/g-C_3N_4 modified ITO electrode *via* interaction between the –COOH groups on the surface of PAMAM dendrimer and the $–NH_2$ groups of peptide and ALP, which can lead to the increase of ALP amount on the modified electrode surface assisted with the PAMAM dendrimer. As a result, the amount of ALP catalyzes of *L*-ascorbic acid 2-phosphate trisodium salt (AAP) to produce electron donor of ascorbic acid (AA), resulting an increased photocurrent. The proposed detection assay displays high selectivity and low detection limit of 0.048 U/mL (S/N = 3) for PKA activity. This biosensor can also be applied for the evaluation of PKA inhibition and PKA activity assay in cell samples. Therefore, the fabricated PEC biosensor is well potential in PKA activity detection and inhibitor screening.

Introduction

Protein phosphorylation catalyzed by protein kinase is one of the most important post-translational modifications in the process of cellular signal transduction, and it plays an essential regulatory role in many vital biological processes, such as cell cycle progression, apoptosis, growth, differentiation and cellular signal communications. [1-3]. Aberrant protein-phosphorylation states and abnormal expression of kinase activity can result in many human diseases, including immune-deficiencies, Alzheimer's disease, cancer, diabetes and cardiovascular and inflammatory diseases [4-6]. Therefore, monitoring protein kinase activity is significant for fundamental biochemical research, clinical diagnosis, and kinase-targeted drug discovery.

Various methods for monitoring protein kinase activities, such as fluorescent, surface-plasmon resonance technique, colorimetric, luminescence resonance energy transfer, mass spectrometric approaches electrogenerated chemiluminescence, electrochemistry, and PEC assays have been proposed [7-14]. Though these assays are effective, a majority of these methods require multi-step detection procedures or expensive recognition proteins. However, it is noteworthy at this point that among these detecting PKA activity assays, PEC method has attracted strong interest due to its low background, simple instrument and excellent sensitivity [15, 16]. For instance, Yan et al. proposed a novel visible-light PEC biosensor based on localized surface plasmon resonance enhancement and dye sensitization for detecting protein kinase activity and its inhibitors [17]. Li et al. investigated the PKA activity assay by fabricating the PEC biosensor based on phosphorylated graphite-like carbon nitride [18].

Yin et al. developed a sensitive and selective PEC assay for monitoring PKA activity based on visible-light active g-C_3N_4 and the specific recognition utility of Phos-tag for PKA-induced phosphopeptides [14]. However, among these PEC strategies, PKA phosphorylation is achieved on the surface of the electrode, which causes some disadvantages, such as rather complex procedure and inadequate contact in reactants. To overcome these defects, in our work, a novel PEC assay is proposed based on accomplishing PKA-catalyzed phosphorylation reaction in solution.

In the PEC sensors, the photoactive materials play a vital role. Thus, metal-free, hazardous-free to environment and excited by visible light photoactive materials are much preferred. Recently, g-C_3N_4, as a metal-free and inorganic polymeric semiconductor material, has attracted tremendous attention [19]. g-C_3N_4 has a typical graphite-like layered structure and possesses the strong covalent bonding within adjacent C-N layers. What's more, due to the sp^2 hybridization, the formation of the *p*-conjugated graphitic planes is the key to making g-C_3N_4 possessing the smallest direct band gap width of 2.7 eV [20, 21], which results in the chemical and thermal stability and an outstanding photocatalyst with visible light irradiation (λ<460 nm). Therefore, due to its excellent chemical and thermal stability, unique semiconductor properties, visible-light response and the merits of metal-free, easy preparation, g-C_3N_4 has been widely applied in the fields of photocatalysis [22] and PEC biosensor [23].

Thus, in our work, we take advantage of the properties of g-C_3N_4 photoactive material to detect PKA activity. In addition, it has been reported that TiO_2 can specifically bind with phosphate groups on substrate peptide [24]. Based on it, TiO_2/g-

C_3N_4 has been synthesized, which plays a role for conjugating phosphate groups and providing PEC signals. More important, to date, no PEC biosensor has been fabricated for achieving PKA-catalyzed phosphorylation reaction in solution. To this end, we develop a simple and sensitive PEC strategy for detecting PKA activity based on combining the PKA-catalyzed phosphorylation reaction in solution with signal amplification of PAMAM dendrimer and ALP. This strategy performs its advantages in two aspects. On the one hand, the PKA-catalyzed phosphorylation reaction is achieved in solution for the virtue of the good contact in reactants and simple experimental procedure. On the other hand, PEC biosensor performs high sensitivity, low background current and simple instrument. What's more, the assay can be further applied to screen PKA inhibitor.

Experimental Section

Reagents and instruments

The substrate peptide (NH_2-LRRASLC-COOH), ALP and adenosine 5'-triphosphate (ATP) disodium salt hydrate were provided by Sangon Biotech Co., Ltd (Shanghai). Carboxypeptidase Y (CPY) and G 3.5 PAMAM dendrimer (generation 3.5, the terminal is –COOH, named as PAMAM-COOH) were obtained from Sigma-Aldrich (USA). PKA catalytic subunit, casein kinase I (CK1), casein kinase II (CK2) and mitogen-activated protein kinase (MAPK) were purchased from New England Biolabs Ltd. (Beverly, MA). $SM(PEG)_{24}$ was obtained from Thermo Fisher Scientific Inc. (USA). Amino-coated magnetic beads (NH_2-MBs) were supplied by Seebio Biotech, Inc. (Shanghai, China). AAP was purchased from DiBo Chemical

Technology co., Ltd. (Shanghai, China). Tris(hydroxymethyl) aminomethane (Tris), tris(2-carboxyethyl) phosphine hydrochloride (TCEP) and AA were supplied by Aladdin (Shanghai, China). Indium Tin Oxide (ITO, coating 180 ± 25 nm, sheet resistance < 15Ω/cm^2) slices were provided by Zhuhai Kaivo Electronic Components Co., Ltd. (Zhuhai, China). All other reagents were analytically purity graded and used as received without further purification.

The buffer solutions employed in this work are shown below. Peptide immobilization buffer, 20 mM Tris-HCl, 2.0 mM EDTA, 2.0 mM NaCl, 2.0 mM TCEP (pH = 7.4). PKA reaction buffer, 0.1 mM EDTA, 80 mM ATP, 2 mM DTT, 50 mM Tris-HCl, 10 mM $MgCl_2$, 0.01% Brij 35 (pH = 7.5). CPY reaction buffer, 20 mM Tris-HCl, 10 mM $MgCl_2$, 50 mM KCl (pH=7.5). Washing buffer, 10 mM Tris-HCl (pH = 7.5). Detection buffer, 10 mM Tris-HCl, 10 mM AAP, 0.1 mM $Mg(NO_3)_2$ (pH=9.8). EIS detection buffer, 5 mM $K_3[Fe(CN)_6]$, 5 mM $K_4[Fe(CN)_6$, 0.1 M KCl. All reagents were of analytical purity. All of the aqueous solutions were prepared using redistilled deionized water, which was autoclaved.

Transmission electron microscope (TEM) images were taken with a JEOL-1200EX instrument (Japan). The photocurrent was recorded on a CHI832A electrochemical workstation (CHI instruments, Austin, USA). PEC measurements were carried out with a home-built PEC system with an additional three-electrode system. A modified ITO electrode (0.195 cm^2) was used as the working electrode. A saturated calomel electrode (SCE) and a Pt wire were applied as the reference electrode and the counter electrode. A 500W Xe lamp equipped with optical filter was employed as the

irradiation source to produce the visible light. Electrochemical impedance spectroscopy (EIS) was performed on a CHI660C electrochemical workstation (CHI instruments, Austin, USA).

Preparation of g-C_3N_4 and TiO_2/g-C_3N_4 nanoparticles

g-C_3N_4 was synthesized according to a procedure reported previously [18]. In a typical gradient temperature-elevating method, the alumina crucible containing 6.0 g of dicyandiamide (DCDA) powder was calcined in a tube furnace under ambient pressure in air. The calcination process was as follows. The tube furnace was heated to 220 ºC at a heating rate of 3 $K \cdot min^{-1}$ and kept at 220 °C for 2 h, following which it was further heated to 350 ºC and 550 ºC and maintained at these temperatures for 2 and 4 h, respectively and then it was cooled to 60 °C at a cooling rate of 3 $K \cdot min^{-1}$. The obtained yellow product was washed with deionized water and anhydrous ethanol for several times and dried in vacuum at 60 °C. The final product was ground into powder for further utilization.

The nonaqueous solvothermal synthesis of TiO_2/g-C_3N_4 composites were according to the literature procedure with proper modifications [25]. Typically, 0.966 g of g-C_3N_4 yellow power was added into 60 mL of anhydrous acetone. And then, 2 mL of tetrabutyl titanate was mixed with the above solution while stirring, following which the mixture was maintained further stirring for 30 min at room temperature. Finally, the obtained mixture was transferred into a 100 mL Teflon-lined stainless steel autoclave and maintained at 180 °C for 12 h. After finishing the reaction, the reactor was cooled to room temperature and the as-synthesized product was collected by

centrifugation. Then, the obtained product was washed extensively with anhydrous acetone and deionized water for several times and dried at 70 ℃ under vacuum.

PKA-catalytic phosphorylation in solution

Briefly, 40 μL PKA reaction solution containing different concentrations of PKA, 40 μL of 4X PKA reaction buffer, 40 μL of 4 μM of peptide were mixed in a 1.5 mL plastic centrifuge tube and the mixture solution was incubated for 50 min at 37 ℃ in the biochemical incubator (After completing the reaction, it was named as solution 1). In the meantime, 10 μL of NH_2-MBs (10 mg/mL) was added into 50 μL $SM(PEG)_{24}$ solution (4.5 mg of $SM(PEG)_{24}$ powder was dissolved in 1 mL dimethylsulfoxide) and mixed into a homogeneous solution. Subsequently, the mixture was shaken for 1 h with ambient condition, which is contributed to N-hydroxysuccinimide ester of $SM(PEG)_{24}$ crosslinker covalent conjugation with amino on surface of the NH_2-MBs (marked as $SM(PEG)_{24}$-MBs). After that, the mixture was separated on a magnet and rinsed with double distilled deionized water for three times to remove the unreacted $SM(PEG)_{24}$. Subsequently, the magnetic fraction was mixed with solution 1 and was further shaken for 1 h, which contributed that peptide can be capture on $SM(PEG)_{24}$-MBs *via* the interaction between the maleimide groups of $SM(PEG)_{24}$ and sulfhydryl of peptide (marked as peptide-$SM(PEG)_{24}$-MBs). Afterwards, the mixture was magnetically separated and washed three times with washing buffer，which separated the peptide from the solution containing abundant ATP and ADP. The obtained magnetic fraction was mixed with 20 μL of CPY (100 μg/mL, dissolved into 20 mM Tris-HCl, 10 mM $MgCl_2$, 50 mM KCl, pH 7.5) and the mixture was incubated for 50

min at 30 °C in the biochemical incubator. After finishing the reaction, the mixture was magnetically separated and the obtained supernatant was named as solution 2, which separated the P-peptide from peptide-SM$(PEG)_{24}$-MBs by hydrolysis of CPY.

Biosensor fabrication

The ITO conductive glasses were used as the working electrode, which were cleaned by acetone, NaOH solution (1 M, in ethanol and distilled water with v/v = 1:1) and distilled water with sonication for 15 min, followed by washing thoroughly with distilled water and then dried at room temperature naturally before it was used.

TiO_2/g-C_3N_4 powder (2 mg) was weighed accurately and dispersed ultrasonically in 1 mL of double distilled deionized water, and then 20 μL of the suspension was dropped onto a piece of ITO electrode. After being dried under infrared lamp, the TiO_2/g-C_3N_4/ITO was rinsed with double distilled deionized water for three times. Then, 20 μL of solution 2 was further dropped on TiO_2/g-C_3N_4/ITO electrode surface and incubated for 30 min in a humid chamber at ambient temperature, followed by rinsed with washing buffer for three times to remove the un-immobilized peptide (The electrode was named as P-peptide/TiO_2/g-C_3N_4/ITO). Subsequently, 20 μL PAMAM-COOH was dropped on P-peptide/TiO_2/g-C_3N_4/ITO electrode surface and incubated for 1 h in a humid chamber at ambient temperature (The –COOH on the surface of PAMAM has been activated by using EDC/NHS solution). After rinsed with washing buffer to remove the un-immobilized PAMAM-COOH for three times, the obtained electrode was noted as PAMAM/P-peptide/TiO_2/g-C_3N_4/ITO. Then, 20 μL EDC/NHS solution was dropped on the electrode surface and incubated for 1 h in a humid

chamber at ambient temperature for activating carboxyl groups of PAMAM-COOH. The obtained electrode was rinsed with washing buffer for three times. Afterwards, 20 μL of ALP solution was dropped onto the PAMAM/P-peptide/TiO_2/g-C_3N_4/ITO electrode for 1 h in a humid chamber at ambient temperature. The obtained electrode (named as ALP/PAMAM/P-peptide/TiO_2/g-C_3N_4/ITO) was rinsed for three times with washing buffer. Finally, the ALP/PAMAM/P-peptide/TiO_2/g-C_3N_4/ITO electrode was inserted in detection buffer 2 and incubated for 1 h at 30 °C in the biochemical incubator, followed by detecting with a home-built PEC system.

For inhibiting the activity of PKA, different concentrations of ellagic acid were introduced into the PKA reaction solution and incubated for 50 min at 37 °C. Then the biosensor was fabricated as described above. The inhibition percent was calculated with the equation of inhibition percent (%) = $(I_1-I_2)/I_1\times100\%$, where I_1 and I_2 was the photocurrent of the biosensor without and with inhibition.

Cell culture and total protein extraction

The process for culturing of human hepatic cell line L-02 and human hepatoma carcinoma cell line HepG2 and extracting total protein from these cells were according to our previous report [26].

Result and discussion

Dectection strategy

In the assay, LRRASLC, containing the recognition sites of PKA (RRASL), was selected as the substrate peptide, in which the hydroxyl group of serine residue could be replaced by γ-phosphoryl from ATP under the catalysis of PKA. As shown in

scheme 1, PKA phosphorylation was achieved in solution instead of on the surface of the electrode, which mainly showed its advantages of the good contact in reactants and simple experimental procedure.

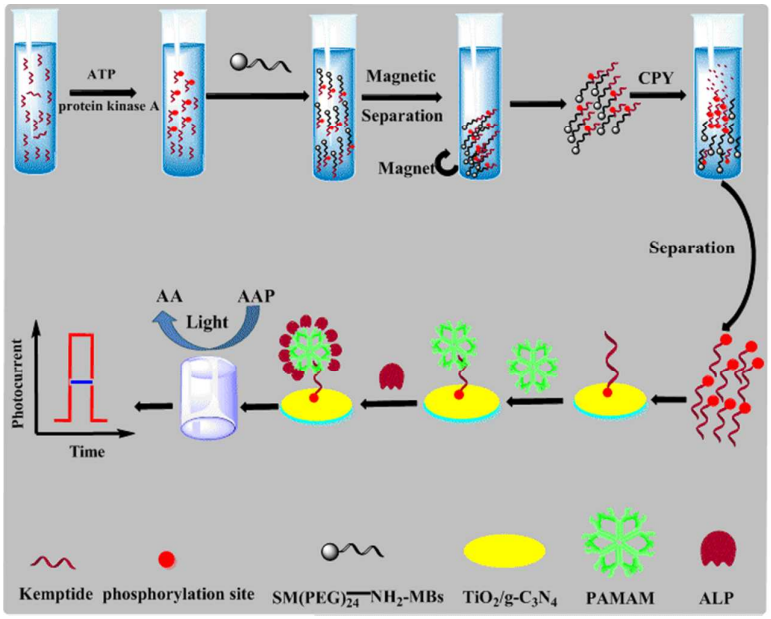

Scheme 1. Schematic representation of the fabricated PEC biosensor for assay of PKA activity based on PKA-catalyzed phosphorylation reaction in solution and signal amplification of TiO_2/g-C_3N_4, PAMAM-COOH and ALP.

In addition, to separate substrate peptide from the solution containing abundant ATP and ADP, $SM(PEG)_{24}$ crosslinker was introduced and it is an amine-to-sulfhydryl crosslinker, which acts as a bridge. $SM(PEG)_{24}$-MBs was obtained by $SM(PEG)_{24}$ integrating specifically and efficiently with amino groups of the NH_2-MBs form stable amide bonds on end. Subsequently, peptide-$SM(PEG)_{24}$-MBs was obtained by $SM(PEG)_{24}$-MBs reacting sulfhydryls of the substrate peptide form stable thioether bonds on the other end, which was magnetically separated from the solution

containing abundant ATP and ADP to avoid disturbing from phosphate groups of ATP and ADP. Next, CPY was used to hydrolyze substrate peptide from the COOH-terminal groups of peptide and the activity could be inhibited when serine residue was phosphorylated by PKA. Therefore, unphosphorylated peptide had been cleaved from the COOH-terminal and released the free amino acid into the solution, and $SM(PEG)_{24}$-MBs were separated from the peptide-$SM(PEG)_{24}$-MBs. Though, the digestion effect of CPY towards the P-peptide could be hindered, $SM(PEG)_{24}$-MBs were separated from the peptide-$SM(PEG)_{24}$-MBs equally. As a result, the P-peptide and the free amino acid were magnetically separated from the peptide-$SM(PEG)_{24}$-MBs. As we all know, TiO_2 can specifically bind with phosphate groups on substrate peptide. Thus, P-peptide could be captured on the surface of TiO_2/g-C_3N_4/ITO. Since the specific peptide is immobilized on TiO_2/g-C_3N_4 nanoparticles only through the phosphate group introduced during the phosphorylation reaction, the quantity of immobilized P-peptide will increase with PKA activity. PAMAM-COOH, generation 3.5 and containing the abundant carboxyl groups, was activated by using EDC/NHS solution, which played a significant role for signal amplification. On the one hand, PAMAM-COOH acted as a bridge between the P-peptide and ALP *via* interaction between the –COOH groups on the surface of PAMAM-COOH and the $–NH_2$ groups of peptide and ALP. On the other hand, a mass of –COOH groups could capture more ALP to reach signal amplification. Thus, the number of immobilized PAMAM-COOH and ALP will increase as a result of the quantity of immobilized P-peptide' increase. Finally, under the catalysis of ALP towards AAP, AA was *in situ* produces as electron

donor. With growing the amount of ALP, the electron donor of AA increased, which resulted in an elevated photocurrent. Therefore, the photocurrent measured will increase with PKA activity. This strategy combined the signal amplification advantages of PAMAM dendrimer and ALP and PKA phosphorylation in solution.

Characterization of TiO_2/g-C_3N_4 composite

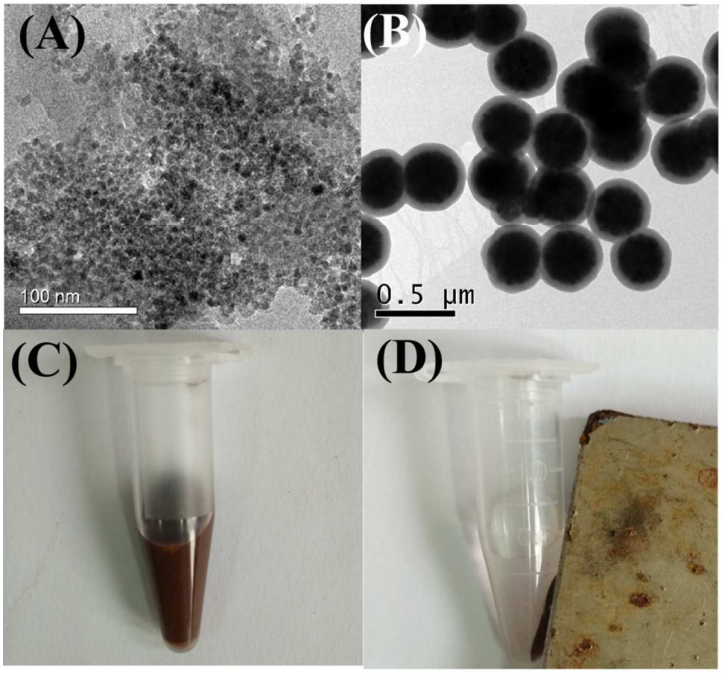

Fig. 1. TEM images of TiO_2/g-C_3N_4 composite (A) and NH_2-MBs (B). Photograph of NH_2-MBs solution (C) and NH_2-MBs attracted towards the magnet for 2s (D).

TiO_2/g-C_3N_4 played a vital role for conjugating phosphate groups and providing PEC signals in the proposed detection method. Fig. 1A revealed the TEM image of TiO_2/g-C_3N_4. And a clearly flat structure with several stacking layers could be clearly observed for g-C_3N_4. What's more, it was worth mentioning that TiO_2 nanoparticles with homogeneous and regular morphology were well dispersed on the surface of g-

C_3N_4, which was favor of TiO_2 binding with P-peptide effectively. Fig. 1B depicted the TEM image of the NH_2-MBs with average diameter of 300 nm, which was consistent with the specification. In addition, the magnetic separability of NH_2-MBs was tested by the experimental observation. As shown in Fig. 1C and Fig. 1D, NH_2-MBs in solution were attracted towards the magnet within 2 s (Fig. 1D), which could be dispersed again like Fig. 1C.

Characterization of the biosensor

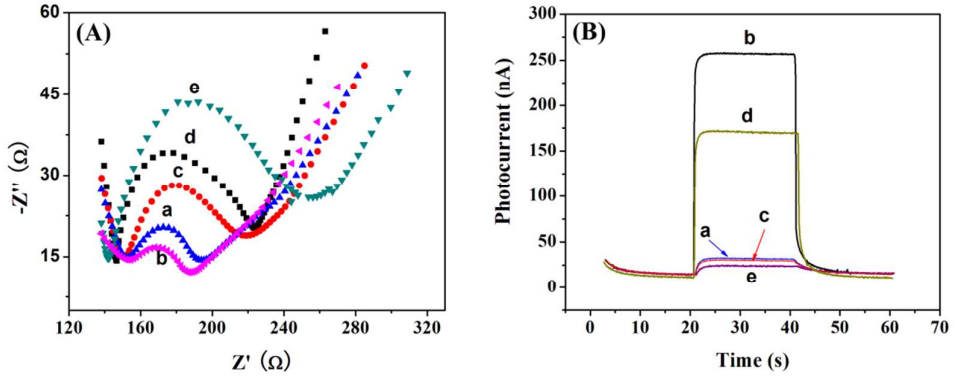

Fig. 2. (A) EIS of ITO (a), TiO_2/g-C_3N_4/ITO (b), P-peptide/TiO_2/g-C_3N_4 /ITO (c), PAMAM/P-peptide/TiO_2/g-C_3N_4/ITO (d) and ALP/PAMAM/P-peptide/TiO_2/g-C_3N_4/ITO (e) in 5 mM $K_3[Fe(CN)_6]/K_4[Fe(CN)_6]$ (1:1) containing 0.1 M KCl. (B) PEC response of different electrodes in 10 mM Tris-HCl, 10 mM AAP, 0.1 mM $Mg(NO_3)_2$ (pH=9.8). (a) TiO_2/g-C_3N_4/ITO, (b) and (d) ALP/PAMAM/P-peptide/TiO_2/g-C_3N_4/ITO with PKA concentration of 50 (b) and 5 (d) U/mL, respectively. (c) The biosensor fabricated without PKA catalysis process, (e) the biosensor fabricated without PAMAM.

The PEC biosensor was fabricated according to Scheme 1 and the modification

process was characterized by EIS in 5 mM $K_3[Fe(CN)_6]/K_4[Fe(CN)_6]$ (1:1) solution containing 0.1 M KCl with the frequency from 10^{-1} to 10^5 Hz. As depicted in Fig. 2A, the bare ITO electrode showed a semicircle with an electron transfer impedance (R_{et}) value about 50 Ω (curve a). However, the R_{et} value decreased to 30 Ω after TiO_2/g-C_3N_4 was immobilized onto ITO electrode surface (curve b), which could be explained as that the immobilization of TiO_2/g-C_3N_4 increased effective surface area of the electrode, improving the diffusion efficiency of the redox probe to electrode and the amino group of g-C_3N_4 nanosheet could promote the diffusion of negative charged redox probe of $Fe(CN)_6^{3-/4-}$ to electrode surface. Subsequently, the R_{et} value increased greatly when the P-peptide was immobilized on the TiO_2/g-C_3N_4/ITO electrode surface, which could be associated with the fact that the P-peptide not only increased the steric hindrance of TiO_2/g-C_3N_4/ITO but also suppressed the diffusion of negative charged redox probe of $K_3[Fe(CN)_6]/K_4[Fe(CN)_6]$ to electrode surface. Afterwards, the R_{et} value further increased when PAMAM-COOH and ALP were captured on the P-peptide/TiO_2/g-C_3N_4/ITO electrode surface consecutively (curve d and curve e), which could be ascribed to the steric hindrance effect of PAMAM-COOH and ALP and carboxyl on the surface of PAMAM-COOH suppressing the diffusion of negative charged redox probe of $K_3[Fe(CN)_6]/K_4[Fe(CN)_6]$ to electrode surface. These changes in the EIS could verify that the PEC biosensor was successfully fabricated.

Detection feasibility assay

To prove the detection feasibility, the photocurrent was compared with different

biosensors in 10 mM Tris-HCl, 10 mM AAP, 0.1 mM $Mg(NO_3)_2$ (pH=9.8). As seen in Fig. 2B, the TiO_2/g-C_3N_4/ITO electrode only presented a weak photocurrent of 17.84 nA (curve a), which could be attributed to the absence of electron donor. However, a strong photocurrent with 242.8 nA was achieved for ALP/PAMAM/P-peptide/TiO_2/g-C_3N_4/ITO (curve b). In the presence of ALP, AAP could be hydrolyzed to produce electron donor of AA, which could denote electron to capture the photo-generated hole and increase the PEC response. When no PKA was added into the reaction system as described in section of PKA-catalytic phosphorylation in solution, the biosensor only showed a weak PEC response with photocurrent of 15.46 nA (curve c), which was greatly lower than that at ALP/PAMAM/P-peptide/TiO_2/g-C_3N_4/ITO. Without PKA, the phosphorylation reaction could not proceed, and no peptide could be modified on the electrode surface. Therefore, no AA could be produced in the detection buffer. Based on the above investigation, the developed method can be applied to detect PKA activity. For further proving the detection feasibility, PKA concentration was changed from 50 (curve b) to 5 (curve d) U/mL. Correspondingly, the photocurrent was decreased from 242.8 to 171.4 nA. The reduced PKA concentration could decrease the phosphorylation level of peptide, which could further result in the low immobilization mount of phosphorylated peptide fragment on the electrode surface, and reduce the capture amount of ALP. Consequently, the amount of AA reduced, which led to a decreased photocurrent. These results also demonstrated that the developed method can be used to detect PKA activity.

For demonstrating the signal amplification role of PAMAM dendrimer in the

developed method, the photocurrent of the biosensor fabricated with and without PAMAM dendrimer was compared, which was also shown in Fig. 2B. The photocurrent of the biosensor fabricated without PAMAM dendrimer (curve e) was 10.12 nA, which was much lower than that obtained at ALP/PAMAM/P-peptide/TiO_2/g-C_3N_4/ITO (curve b). According to Scheme 1, ALP could not be captured on electrode surface without PAMAM, which would further lead to the failure of the hydrolysis of AAP to generate electron donor of AA. Therefore, only a weak photocurrent was obtained. The amplification factor (k) is estimated to be 24 approximately ($k = I_2/I_1$, where I_1 is the photocurrent of the biosensor fabricated in the absence of PAMAM dendrimer, and I_2 is the photocurrent of the biosensor fabricated integratedly). This result indicated that PAMAM dendrimer played a significant role in the signal amplification assay.

Optimization of TiO_2/g-C_3N_4 composite concentration and PKA catalysis time

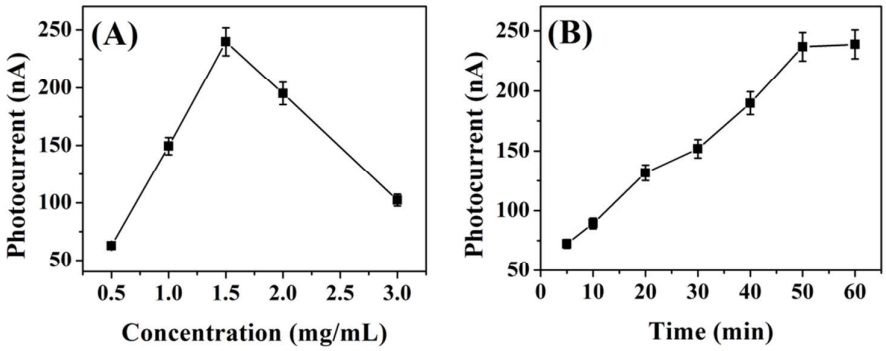

Fig. 3. The effect of TiO_2/g-C_3N_4 concentration (A) and PKA catalysis time on the PEC response of the biosensor. PKA concentration is 50 U/mL (B).

In this developed PEC biosensor, TiO_2/g-C_3N_4 was used as the PEC signal probe

and P-peptide capture reagent. Thus its concentration could significantly influence the photocurrent intensity and the detection sensitivity. Fig. 3A showed the effect of TiO_2/g-C_3N_4 concentration on the PEC response. With increasing the concentration of TiO_2/g-C_3N_4 from 0.5 to 1.5 mg/mL, the photocurrent increased gradually. When further enhancing TiO_2/g-C_3N_4 concentration, the photocurrent decreased reversely, which could be explained as that the thick film of TiO_2/g-C_3N_4 could improve the electron transfer resistance and decrease the photocurrent. Thus, 1.5 mg/mL of TiO_2/g-C_3N_4 concentration was selected.

To assess the effect of PKA catalysis time on the PEC response, the phosphorylation process catalyzed by PKA was performed with different time. As illustrated in Fig. 3B, with increasing phosphorylation time from 0 to 50 min, the photocurrent gradually increased. However, when the phosphorylation time prolonged further, the photocurrent only increased a little and tended to level off. Therefore, 50 min was selected.

PKA activity assay

Under the optimal experimental conditions, the relationship between the PEC response and PKA concentration was investigated. As shown in Fig. 4A and Fig. 4B, the photocurrent increased with improving PKA concentration from 0.1 to 100 U/mL. The photocurrent showed a linear relationship with the logarithm value of PKA concentration. The linear regression equation can be expressed as I (nA) =71.76log$c$(U/mL)+107.46 (R = 0.9972) and the detection limit is 0.048 U/mL (S/N = 3), which was lower than some of previous reports, as listed in Table 1. In addition,

we have compared the assay time of the developed methods with other methods for PKA activity detection in the Table 1, which indicated that the developed method might be a desired detection strategy for protein kinase activity assay.

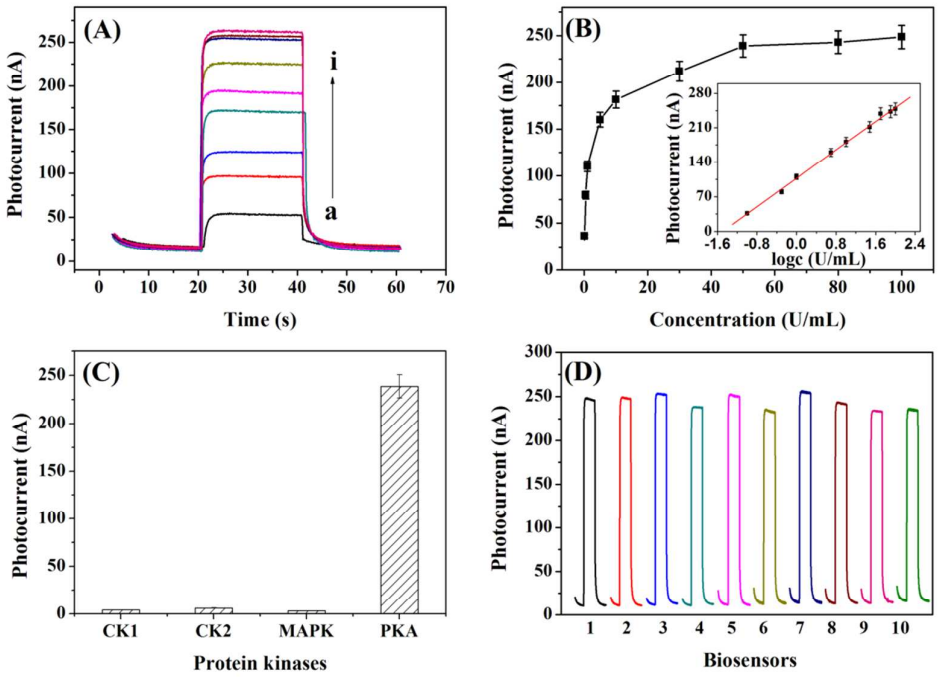

Fig. 4. (A) The PEC response of the biosensor with different PKA concentrations. a-i: 0.1, 0.5, 1, 5, 10, 30, 50, 80, 100 U/mL. (B) The plot for the quantity of PEC versus PKA concentration. The insert is the linear relationship between the PEC intensity and the logarithm of PKA concentrations. (C) The PEC intensity change after the biosensor was incubated with 50 U/mL different kinases. (D) The PEC response of ten biosensors fabricated independently. PKA concentration is 50 U/mL.

In order to explore the good selectivity of the fabricated biosensor, three kinds of protein kinases (MAPK, CK1 and CK2, which cannot recognize the substrate peptide of RRASLC) were selected as the model interferents. And the photocurrent change

($\Delta I = I_1$-I_2) of the biosensor fabricated with different protein kinases was compared, where I_1 was the PEC intensity of the biosensor with 50 U/mL different protein kinase and I_2 was the PEC intensity with 0 U/mL protein kinase. As depicted in Fig. 4C, that the ΔI of the biosensor fabricated with MAPK, CK1 and CK2 were much lower than that PKA, indicating that the developed biosensor had good detection specificity. The reproducibility of the proposed PEC method had been evaluated by ten repeatedly prepared biosensors. As seen in Fig. 4D, the relative standard deviation was 3.88%, indicating that the developed method displayed acceptable reproducibility.

Table 1. The comparison of the detection performance and the assay time of the developed PEC assay with other methods for kinase activity

Methods	Kinase	Linear range (U/mL)	LOD (U/mL)	The assay time (h)	Refs.
Fluorescence	PKA	0-1000	0.5	~3	[27]
Fluorescence	PKA	0-800	0.47	~3	[28]
Fluorescence	PKA	0.5-1000	0.1	~3	[24]
FRET	PKA		0.08	~15	[29]
Electrochemistry	PKA	0.1-1	0.09	~18	[30]
PEC assay	PKA	0.05-50	0.077	~38	[18]
ECL	PKA	0.07-32	0.07	~18	[11]
QCM	PKA	0.64-22.33	0.061	~20	[31]
PEC assay	PKA	0.05–100	0.048	~9	This work

ECL: electrochemiluminescence; QCM: quartz crystal microbalance; FRET: fluorescence resonance energy transfer.

Inhibition assay

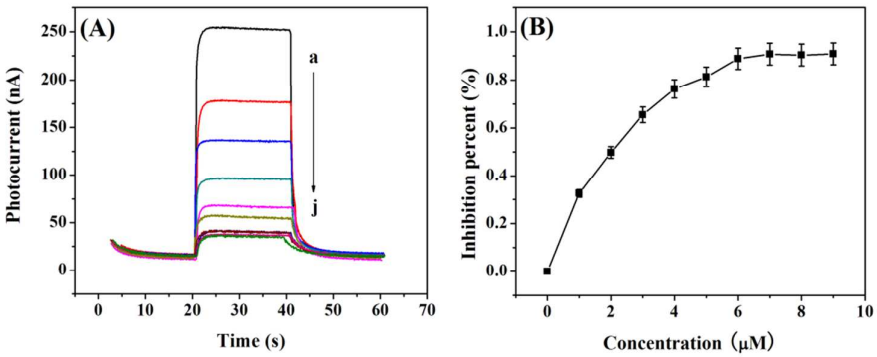

Fig. 5. (A) PEC response of the biosensor in the presence of different concentrations of ellagic acid. a-j: 0, 1, 2, 3, 4, 5, 6, 7, 8 and 9 μM. PKA concentration is 50 U/mL. (B) The plot for the relationship between ellagic acid concentration and inhibition percent.

Protein kinase inhibitors may have a significant impact on inhibiting protein kinase activity and become potential drugs. Thus, protein kinase inhibitor screening had attracted strong interest and it has also been investigated in this work. To test the potential application of our proposed PEC strategy in PKA inhibitor screening, ellagic acid, a well-recognized efficient PKA inhibitor, was selected as a model inhibitor. The PEC intensity of the fabricated biosensor by mixing 50 U/mL PKA and different concentrations of ellagic acid was observed in Fig. 5A. Since the activity of PKA reduces with increasing of the concentrations of ellagic acid, the quantity of immobilized P-peptide and the photocurrent measured will decrease as a result of the PKA activity' decrease. And the inhibition effect of ellagic acid on PKA activity was acquired in Fig. 5B. As shown in Fig. 5B, as the ellagic acid concentration was increased, there was an increase in inhibition percent. The maximum inhibition

percent of PKA activity was observed when treated with 7 μM ellagic acid. The IC_{50} value (the half-maximal inhibitory concentration required to reduce enzyme activity by 50%) of ellagic acid was found to be 2.1 μM, which was close to the previously reported value of 1.66 μM [32] and 2.5 μM [33]. The result suggests that the developed PEC biosensor could be applied in the field of screening the PKA inhibitor.

Detection of PKA in real samples

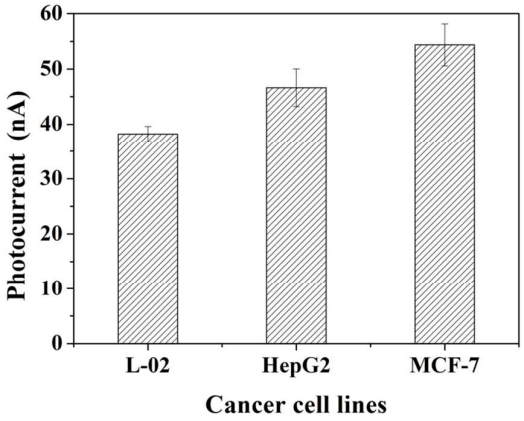

Fig. 6. The histogram for PKA activity in different cancer cell lines.

Overexpression of protein kinase has been associated with cancer cell and PKA is a kind of potential cancer biomarker for early diagnosis and prognostics [34]. However, the content of PKA in human cells is very low [17, 35, 36], so the sensitive detection method is needed to investigate the relationship between the express level change of PKA and cancer. To evaluate the applicability of the developed method for PKA detection in biological samples, the PKA activity was compared in human hepatocyte cell line L-02, human hepatoma carcinoma cell line HepG2 and human breast cancer cell line MCF-7. As can be seen in Fig. 6, PKA activity in HepG2 and MCF-7 was greatly higher than that in L-02, indicating high biological activity of PKA in human

cancer cells. In addition, PKA activity in MCF-7 was also a little higher than that in HepG2, implying different activity of PKA in different cancer cells. These results were in accordance with previous reports [14, 36, 37]. Based on the above investigation, one can conclude that the developed method could be used to detect PKA activity in complex biological samples with high detect sensitivity.

Conclusion

In summary, a novel PEC biosensor is successfully developed for PKA activity detection based on combining the PKA-catalyzed phosphorylation reaction in solution with signal amplification of PAMAM dendrimer and ALP, which performs a highly sensitive detection for PKA activity with a low detection limit of 0.048 U/mL (S/N = 3). In addition, the fabricated PEC biosensor is well potential in detection of PKA activity in biological samples and inhibitor screening, which might be helpful for the discovery of anticancer drugs.

Acknowledgements

This work was supported by the National Key Research and Development Plan (No. 2016YFD0800202), China Postdoctoral Science Foundation (No. 2014M550369，No. 2015M582120), the National Natural Science Foundation of China (No. 21375079).

References

(1) Adams, J. A., *Chem. Rev.* **2001,** *101*, 2271-2290.

(2) Johnson, L. N.; Lewis, R. J., *Chem. Rev.* **2001,** *101*, 2209-2242.

(3) Manning, G.; Whyte, D. B.; Martinez, R.; Hunter, T.; Sudarsanam, S., *Science* **2002,** *298*, 1912-1934.

(4) Vieth, M.; Sutherland, J. J.; Robertson, D. H.; Campbell, R. M., *Drug Discov. Today* **2005,** *10*, 839-846.

(5) Skorski, T., *Nat. Rev. Cancer* **2002,** *2*, 351-360.

(6) Yarden, Y.; Sliwkowski, M. X., *Nat. Rev. Mol. Cell Biol.* **2001,** *2*, 127-137.

(7) Song, Y.; Wei, W.; Qu, X., *Adv. Mater.* **2011,** *23*, 4215-4236.

(8) Gonzalez-Vera, J. A., *Chem. Soc. Rev.* **2012,** *41*, 1652-1664.

(9) Wang, Y.; Yan, B.; Chen, L., *Chem. Rev.* **2013,** *113*, 1391-1428.

(10) Liu, C.; Chang, L.; Wang, H.; Bai, J.; Ren, W.; Li, Z., *Anal. Chem.* **2014,** *86*, 6095-6102.

(11) Xu, S.; Liu, Y.; Wang, T.; Li, J., *Anal. Chem.* **2010,** *82*, 9566-9572.

(12) Liu, J.; He, X.; Wang, K.; He, D.; Wang, Y.; Mao, Y.; Shi, H.; Wen, L., *Biosens. Bioelectron.* **2015,** *70*, 54-60.

(13) Xu, X.; Nie, Z.; Chen, J.; Fu, Y.; Li, W.; Shen, Q.; Yao, S., *Chem. Commun.* **2009**, 6946-6948.

(14) Yin, H.; Sun, B.; Dong, L.; Li, B.; Zhou, Y.; Ai, S., *Biosens. Bioelectron.* **2015,** *64*, 462-468.

(15) Haddache, F.; Le Goff, A.; Reuillard, B.; Gorgy, K.; Gondran, C.; Spinelli, N.; Defrancq, E.; Cosnier, S., *Chem.-Eur. J.* **2014,** *20*, 15555-15560.

(16) Zhao, W.-W.; Xu, J.-J.; Chen, H.-Y., *Chem. Rev.* **2014,** *114*, 7421-7441.

(17) Yan, Z.; Wang, Z.; Miao, Z.; Liu, Y., *Anal. Chem.* **2015,** *88*, 922-929.

(18) Li, X.; Zhou, Y.; Xu, Y.; Xu, H.; Wang, M.; Yin, H.; Ai, S., *Anal. Chim. Acta* **2016,** *934*, 36-43.

(19) Kroke, E.; Schwarz, M., *Coord. Chem. Rev.* **2004,** *248*, 493-532.

(20) Bojdys, M. J.; Müller, J.-O.; Antonietti, M.; Thomas, A., *Chemistry–A European Journal* **2008,** *14*, 8177-8182.

(21) Tian, Y.; Chang, B.; Fu, J.; Zhou, B.; Liu, J.; Xi, F.; Dong, X., *J. Solid State Chem.* **2014,** *212*, 1-6.

(22) Wang, Y.; Wang, X.; Antonietti, M., *Angew. Chem. Int. Ed.* **2012,** *51*, 68-89.

(23) Zhuang, J.; Lai, W.; Xu, M.; Zhou, Q.; Tang, D., *ACS Appl. Mat. Interfaces* **2015,** *7*, 8330-8338.

(24) Bai, J.; Zhao, Y.; Wang, Z.; Liu, C.; Wang, Y.; Li, Z., *Anal. Chem.* **2013,** *85*, 4813-4821.

(25) Tian, Z.; Li, Q.; Li, Y.; Ai, S., *Catal. Commun.* **2015,** *61*, 97-101.

(26) Yin, H.; Wang, X.; Guo, Y.; Zhou, Y.; Ai, S., *Biosens. Bioelectron.* **2015,** *66*, 77-83.

(27) Tan, P.; Lei, C.; Liu, X.; Qing, M.; Nie, Z.; Guo, M.; Huang, Y.; Yao, S., *Anal. Chim. Acta* **2013,** *780*, 89-94.

(28) Xu, X.; Liu, X.; Nie, Z.; Pan, Y.; Guo, M.; Yao, S., *Anal. Chem.* **2011,** *83*, 52-59.

(29) Shiosaki, S.; Nobori, T.; Mori, T.; Toita, R.; Nakamura, Y.; Kim, C. W.; Yamamoto, T.; Niidome, T.; Katayama, Y., *Chem. Commun.* **2013,** *49*, 5592-5594.

(30) Liu, J.; He, X.; Wang, K.; Wang, Y.; Yan, G.; Mao, Y., *Talanta* **2014,** *129*, 328-335.

(31) Xu, X.; Zhou, J.; Liu, X.; Nie, Z.; Qing, M.; Guo, M.; Yao, S., *Anal. Chem.*

2012, *84*, 4746-4753.

(32) Gu, G.; Wang, H.; Liu, P.; Fu, C.; Li, Z.; Cao, X.; Li, Y.; Fang, Q.; Xu, F.; Shen, J., *Chem. Commun.* **2012,** *48*, 2788-2790.

(33) Chen, Z.; He, X.; Wang, Y.; Wang, K.; Du, Y.; Yan, G., *Biosens. Bioelectron.* **2013,** *41*, 519-525.

(34) Stork, P. J.; Schmitt, J. M., *Trends in cell biology* **2002,** *12*, 258-266.

(35) Wang, Z.; Yan, Z.; Sun, N.; Liu, Y., *Biosens. Bioelectron.* **2015,** *68*, 771-776.

(36) Li, T.; Liu, X.; Liu, D.; Wang, Z., *Anal. Chem.* **2013,** *85*, 7033-7037.

(37) Wang, Z.; Sun, N.; He, Y.; Liu, Y.; Li, J., *Anal. Chem.* **2014,** *86*, 6153-6159.

TOC Graph

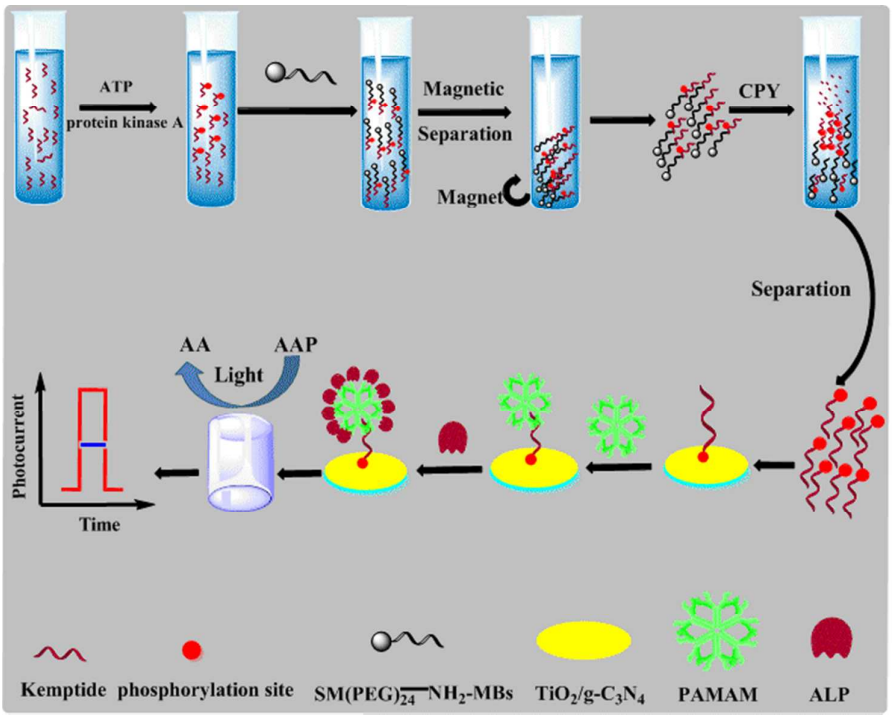
ATP
protein kinase A
Magnetic
Separation
Magnet
CPY
Separation
AA
AAP
Light
Photocurrent
Time
Kemptide
phosphorylation site
SM(PEG)24NH2-MBs
TiO2/g-C3N4
PAMAM
ALP

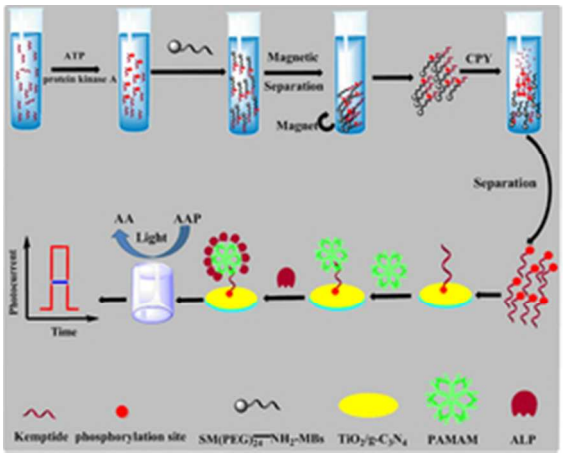

Scheme 1

11x9mm (600 x 600 DPI)

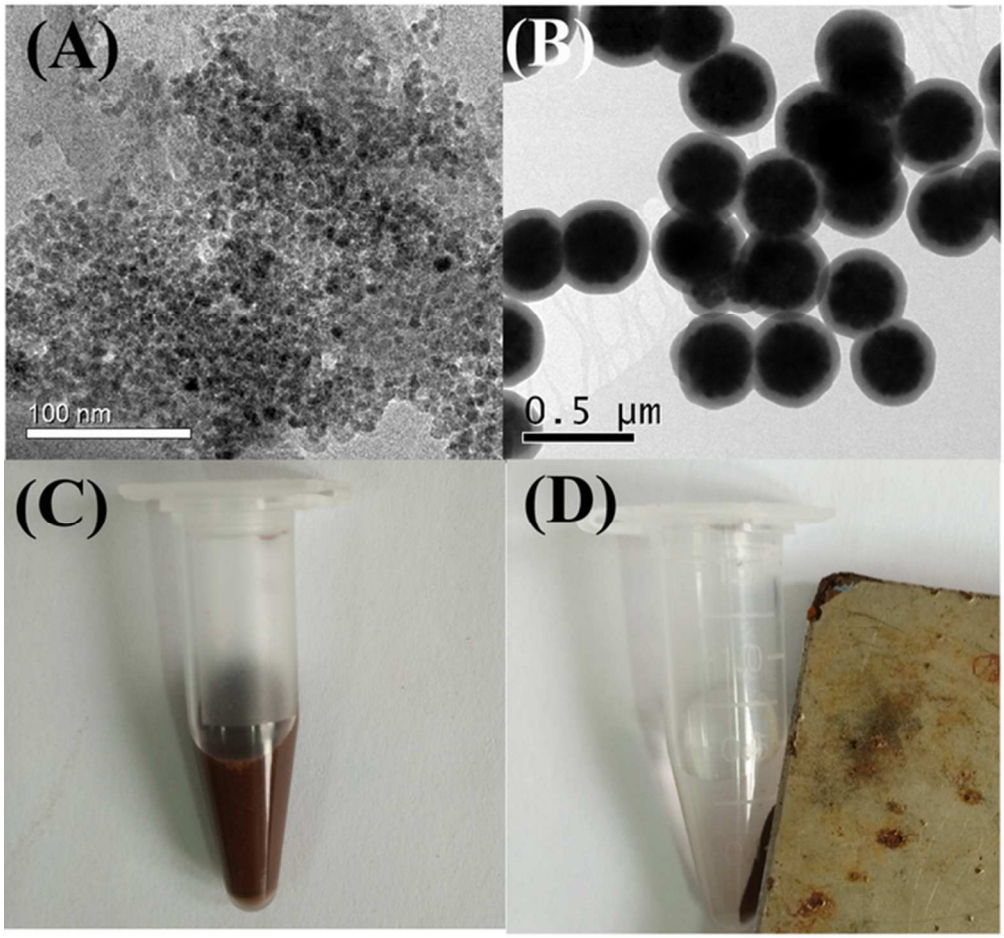

Figure 1

28x27mm (600 x 600 DPI)

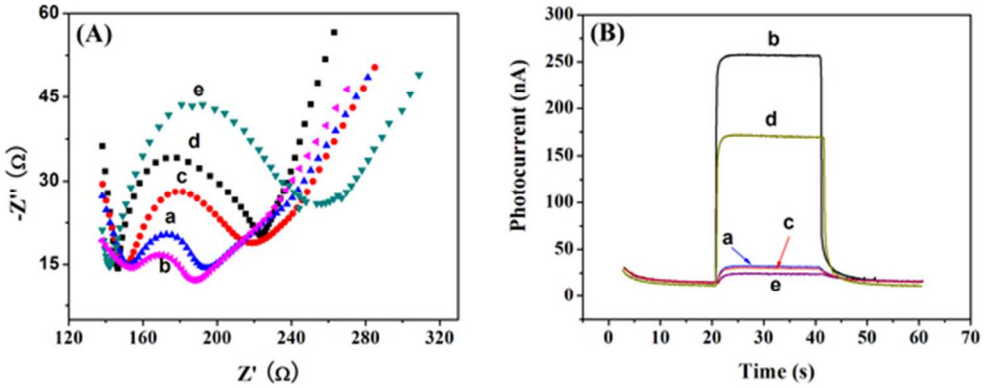

Figure 2

26x10mm (600 x 600 DPI)

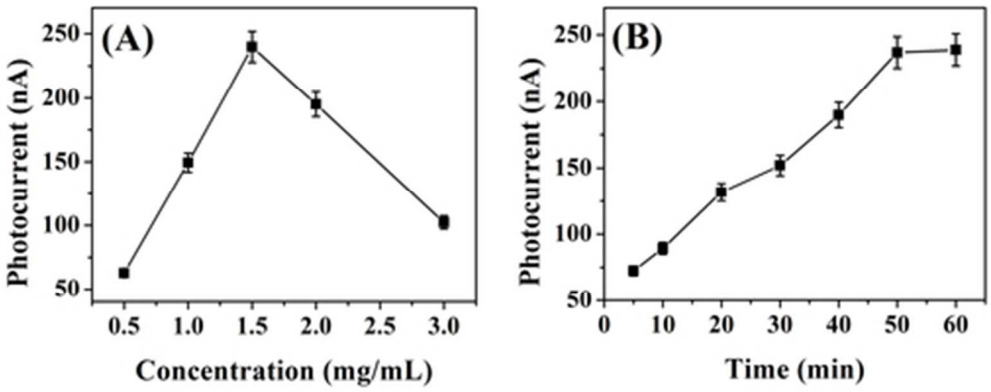

Figure 3

21x8mm (600 x 600 DPI)

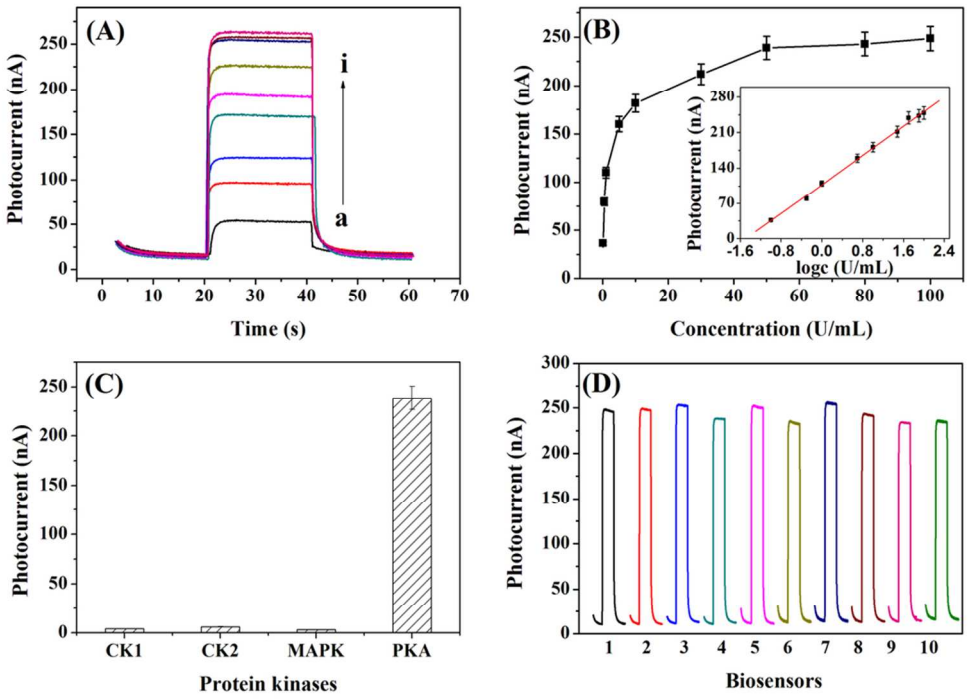

Figure 4

45x32mm (600 x 600 DPI)

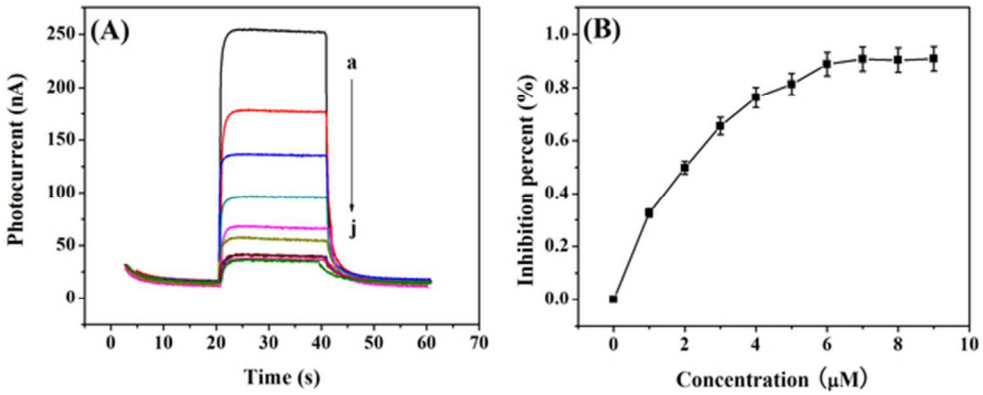

Figure 5

27x11mm (600 x 600 DPI)

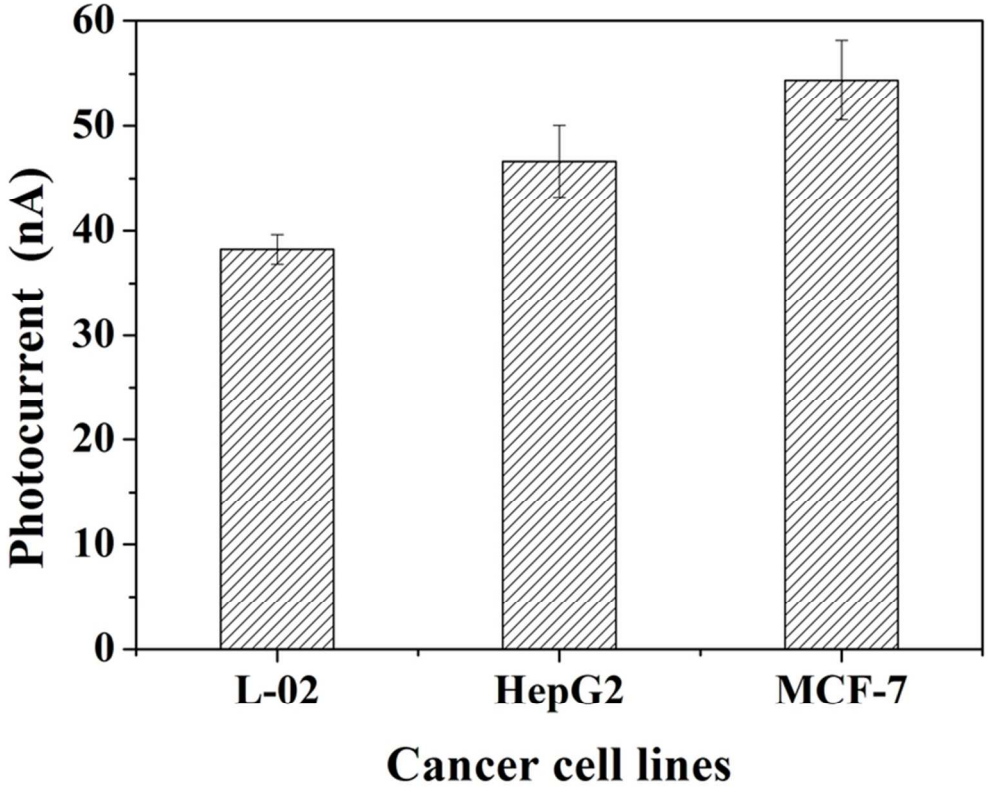

Figure 6

34x27mm (600 x 600 DPI)